8 Supporting information for "North Atlantic temperature change across the Eocene–Oligocene Transition"

Contents of this file

- Section S8.1
- Figure S1 to Figure S16
- Table S1

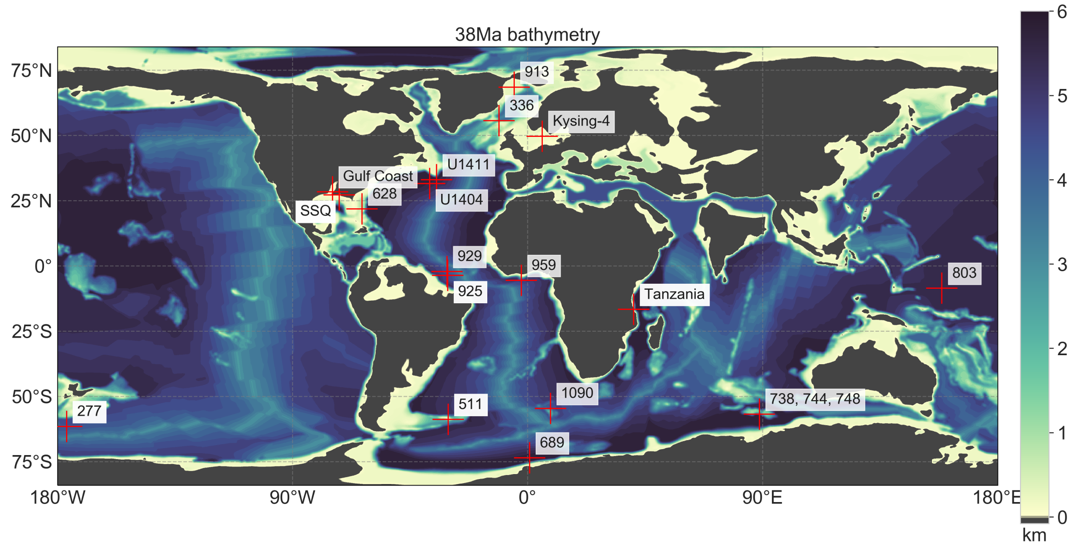

Figure S1. Paleobathymetry of Baatsen et al. (2016) for 38 Ma, with reconstructed drill site locations from the latitudinal composite of Hutchinson et al. (2021).

S8.1 Foraminifera preservation mass-balance calculation

If the foraminifera would have been affected by deep-sea dissolution and recrystallisation, we can estimate how much of the test material would have to be overprinted by a simple mass-balance calculation for the worst-case scenario: assuming deep-sea temperatures (DST) of 0.0 °C (the modern ocean values at this site, so likely warmer during the Eocene) and SST estimates of 28 °C (Liu et al., 2018).

$$\mathrm{SST}_{\mathrm{rec}} = (1 - \alpha)\mathrm{SST} + \alpha\mathrm{DST},$$

(2)

Table S1. Average stable isotope results for the mixed-layer (M) dwelling foraminifera and the thermocline (T) dwelling foraminifera across the EOT.

	Age (Ma)	N	$\delta^{13}C$ (VPDB)	$\delta^{18}O$ (VPDB)	Δ_{47} (‰ I-CDES)	T (°C)	$\delta^{18}O_{sw}$ (VSMOW)
M	32.5	22	0.76 ± 0.081	0.39 ± 0.26	0.63 ± 0.017	13 ± 5.2	0.32 ± 1.4
M	33.6	72	1.5 ± 0.039	0.42 ± 0.06	0.62 ± 0.0073	17 ± 2.3	1.1 ± 0.55
M	33.7	52	0.85 ± 0.046	-0.19 ± 0.071	0.61 ± 0.012	18 ± 3.8	0.79 ± 0.87
M	35.1	43	0.67 ± 0.051	-0.33 ± 0.076	0.61 ± 0.012	18 ± 4	0.61 ± 0.91
T	32.5	28	0.79 ± 0.055	1.3 ± 0.18	0.63 ± 0.016	14 ± 5	1.4 ± 1.3
T	33.6	37	1.3 ± 0.035	1.4 ± 0.1	0.64 ± 0.014	10 ± 4.1	0.6 ± 1
T	33.7	31	0.75 ± 0.034	0.17 ± 0.071	0.63 ± 0.016	14 ± 5	0.32 ± 1.2
T	35.1	24	0.64 ± 0.04	-0.17 ± 0.089	0.61 ± 0.013	20 ± 4.3	1.2 ± 0.98

where SST_{rec} is the reconstructed SST, and thus:

$$\alpha = (SST_{rec} - SST)/(DST - SST). \tag{3}$$

To arrive at our reconstructed Eocene SST of 18 °C, an overprinting of more than 42 % would be required. Figure S2 shows the overprinting factor required under different assumptions for the deep sea temperature (−1.9 °C, the minimum sea water temperature prior to freezing up to 8 °C) and the assumed true SST. Most of these scenarios require at least 10 % overprinting to achieve the clumped-isotope derived temperatures we arrive at. Given the photographic evidence and the previous studies of the excellent preservation at this site (Leutert et al., 2019; Norris et al., 2014), this is highly unlikely.

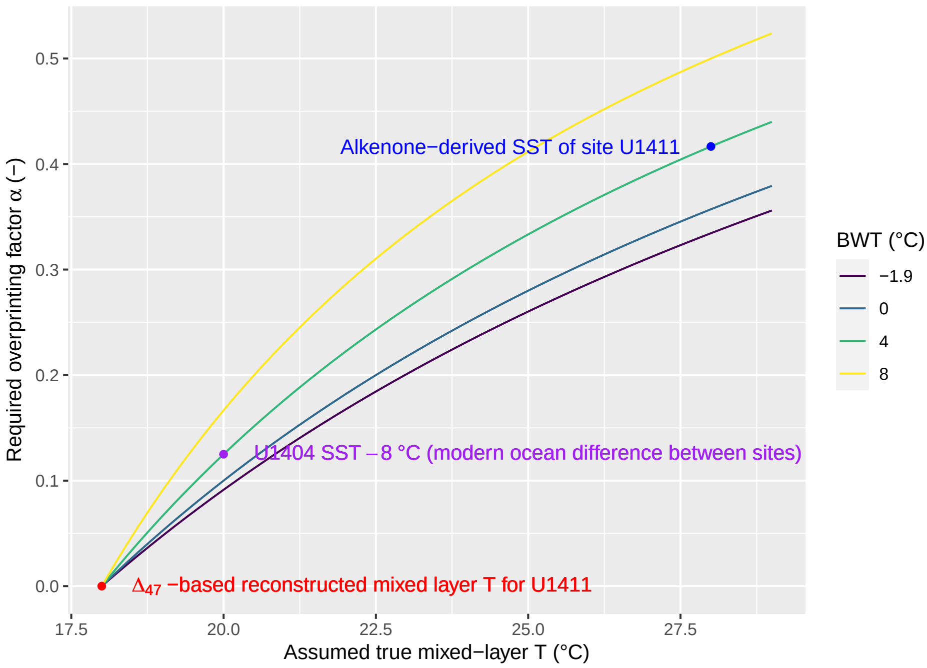

Figure S2. Overprinting factor α required to arrive at final clumped-isotope based temperature under different 'true' sea surface temperature assumptions (x-axis) and bottom water temperature assumptions (colour).

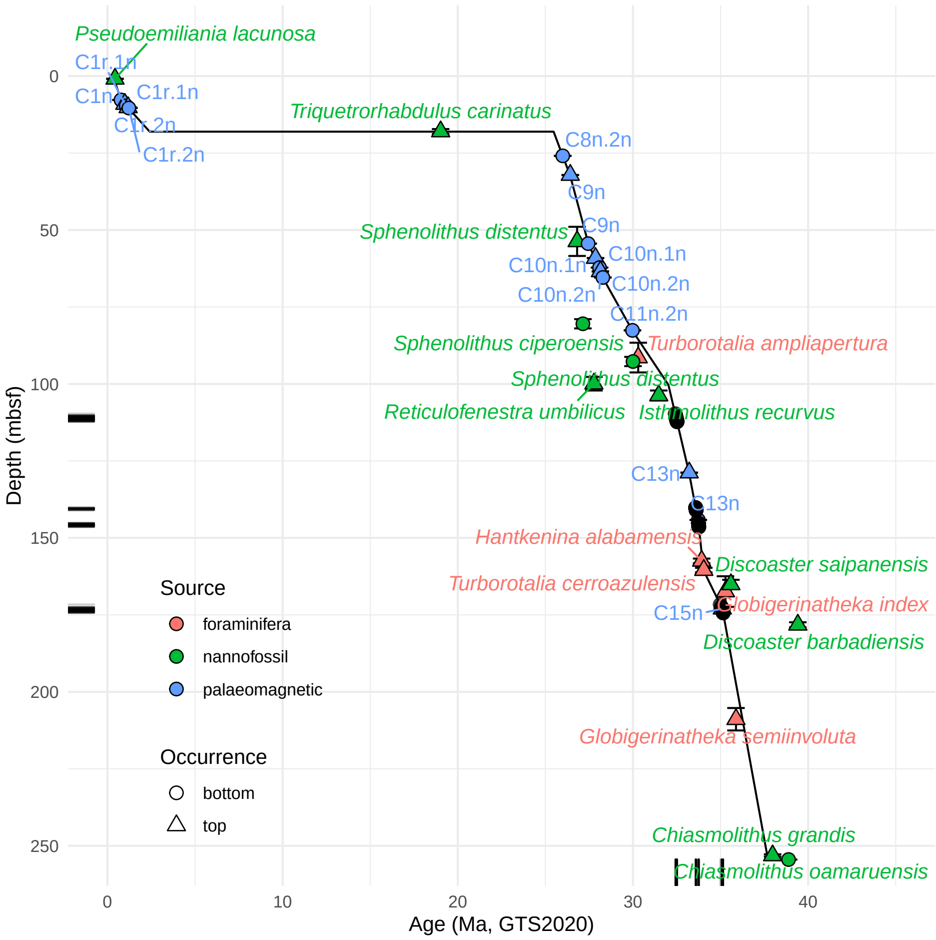

Figure S3. The age model for IODP site U1411 is based on the shipboard age model (Norris et al., 2014) with adjustments from the Neptune database (Renaudie, Lazarus, & Diver, 2020) presented on the Geological Time Scale 2020 (Speijer et al., 2020). The black line represents the age model, with the tops (triangles) and bottoms (circles) of foraminifera (red), nannofossil (green), and magnetic polarity chrons (blue). Black points and segments near the axes represent the samples analyzed in this study.

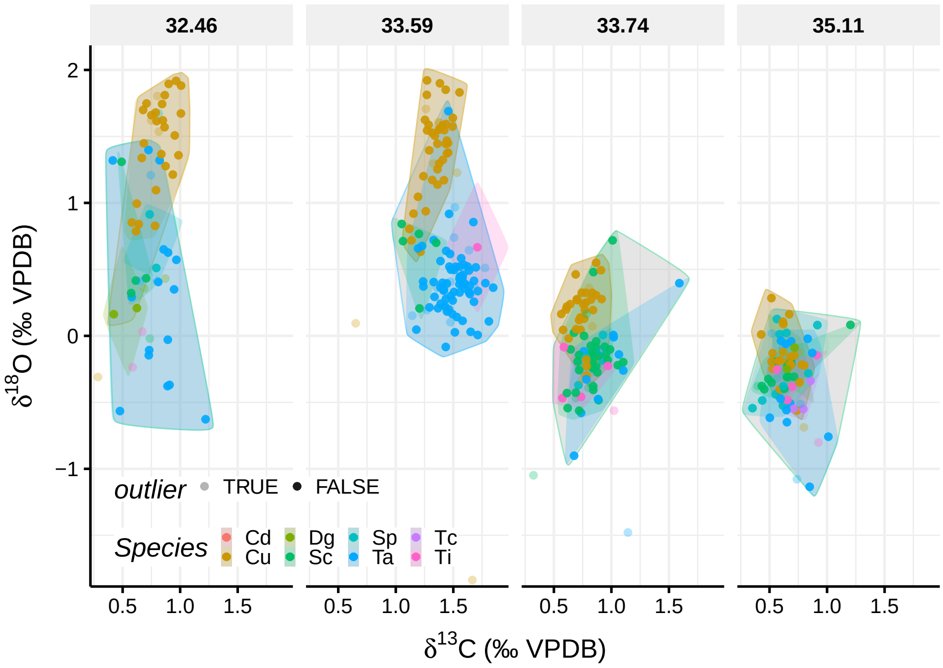

Figure S4. The planktic foraminifera of IODP site U1411 that group together on the δ^{13}C and δ^{18}O scales were averaged for clumped isotope analysis. Columns indicate the average sample time-period in Ma. Cd = *C. dissimilis*, Cu = *C. unicavus*, Dg = *D. galivasi*, Sc = *S. corpulenta*, Sp = *S. projecta*, Ta = *T. ampliapertura*, Tc = , Ti = *T. increbescens*.

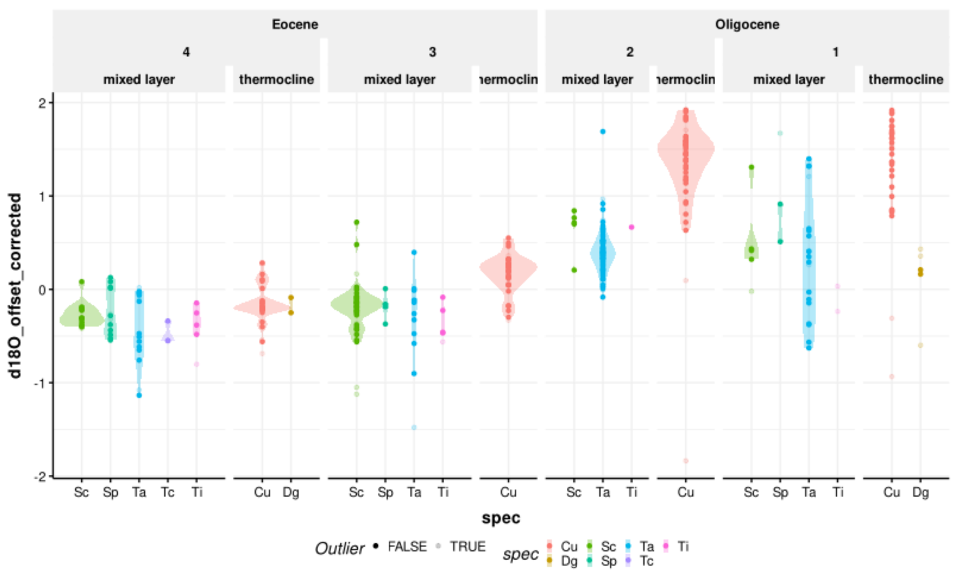

Figure S5. Species assignment based on δ^{18}O values across the 4 sampled intervals. Note that we changed the assigned dwelling depths of *S. corpulenta* and *S. projecta* because they appeared to agree better with *T. ampliapertura* values than with *C. unicavus* (Figure S5).

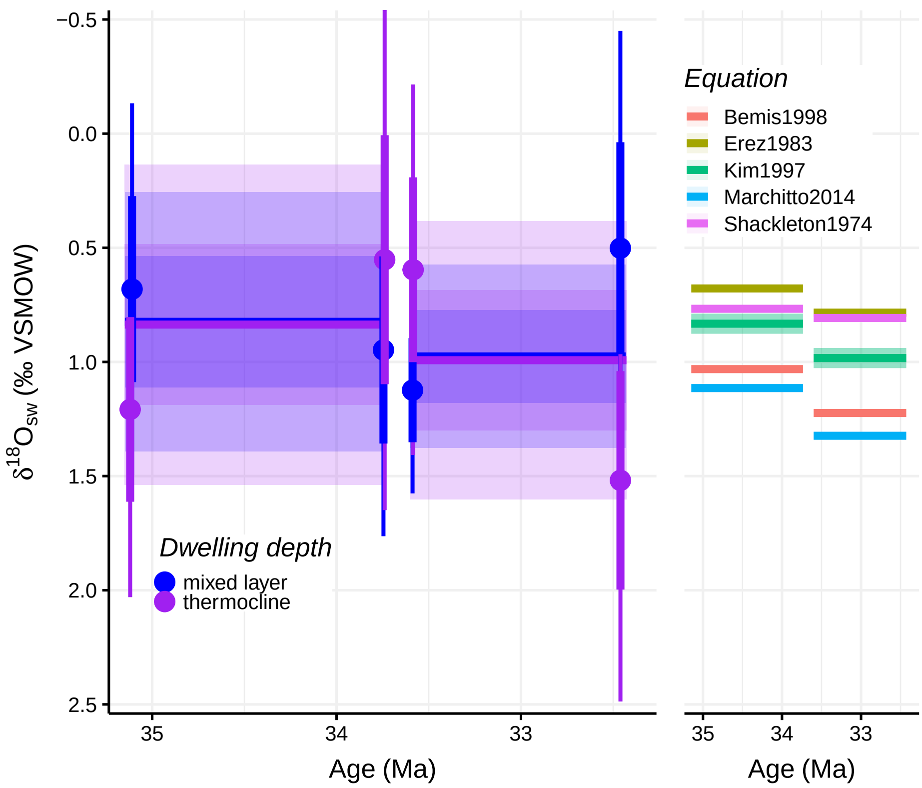

Figure S6. $\delta^{18}O_{sw}$ estimates inherit their large uncertainty from the Δ_{47} temperatures. The right hand panel shows the effect of choosing a different equation that relates $\delta^{18}O_{cc}$ and temperature to $\delta^{18}O_{sw}$ (Bemis et al., 1998; Erez & Luz, 1983; Kim & O'Neil, 1997; Marchitto et al., 2014; Shackleton, 1974). Our preferred equation is highlighted in green.

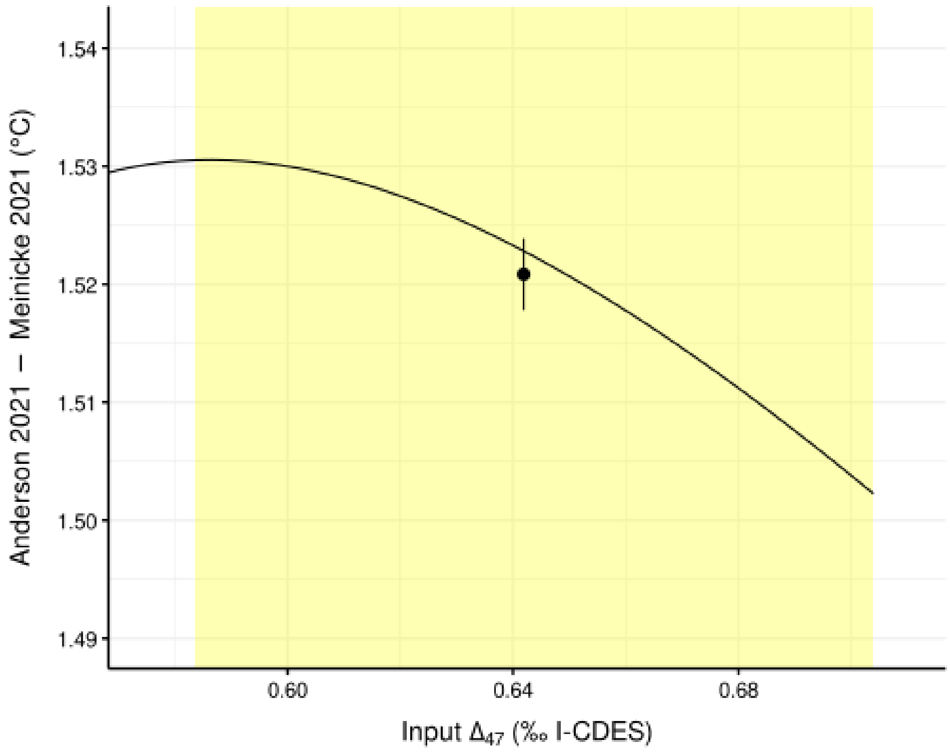

Figure S7. Comparison between the Anderson et al. (2021) and Meinicke et al. (2021) calibrations for the temperature range of interest for palaeoclimate reconstructions (yellow rectangle).

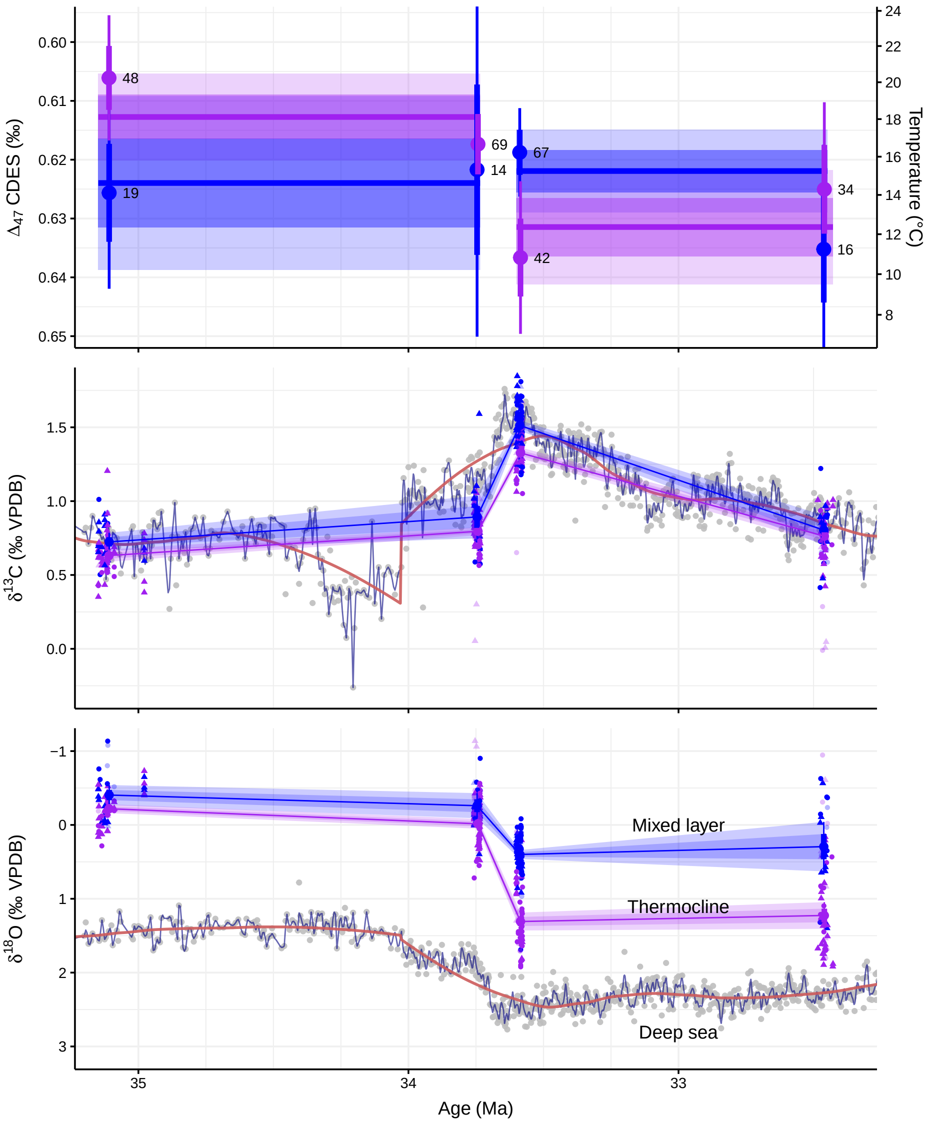

Figure S8. Same as Figure 4, but calculated based on previous depth associations of the different foraminifera species from Table 1.

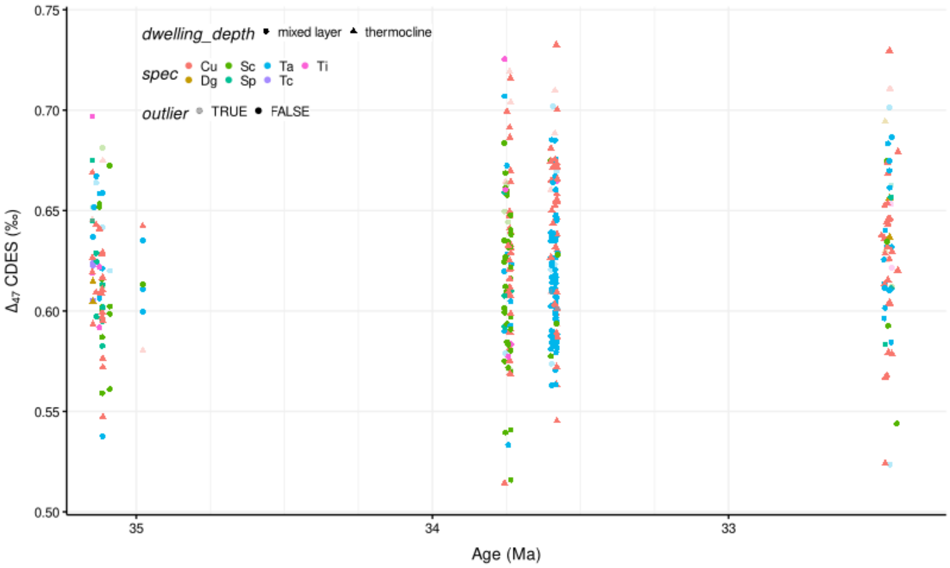

Figure S9. All replicate clumped isotope points used to generate averages.

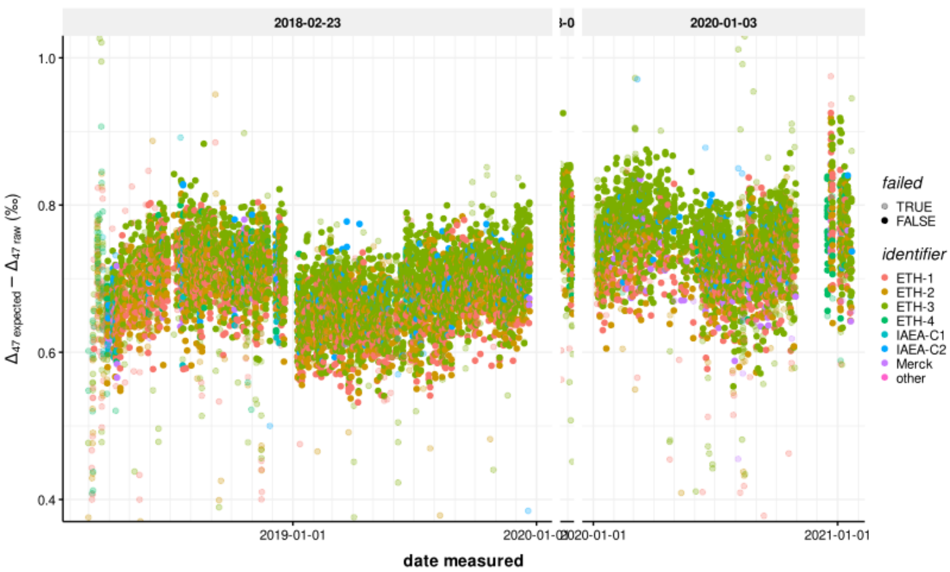

Figure S10. Offset correction criteria for the whole measuement range.

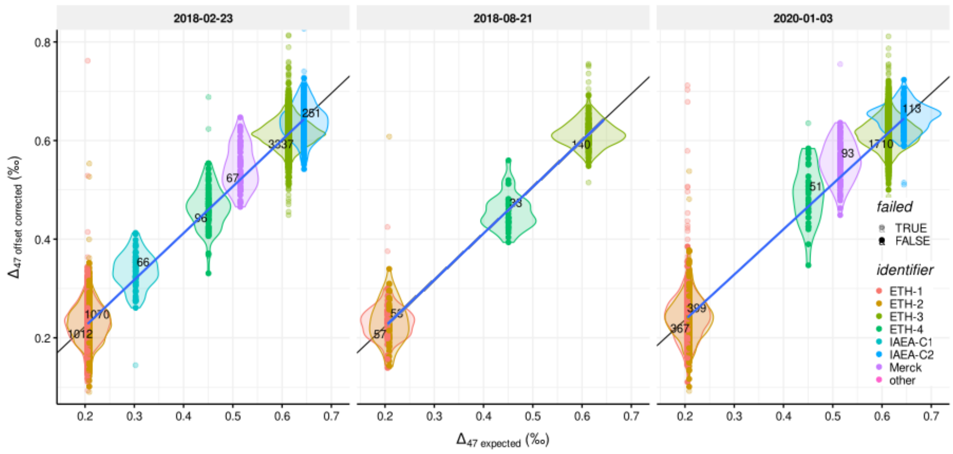

Figure S11. Empirical transfer functions for the sessions at UU (left and right) and at UiB (middle).

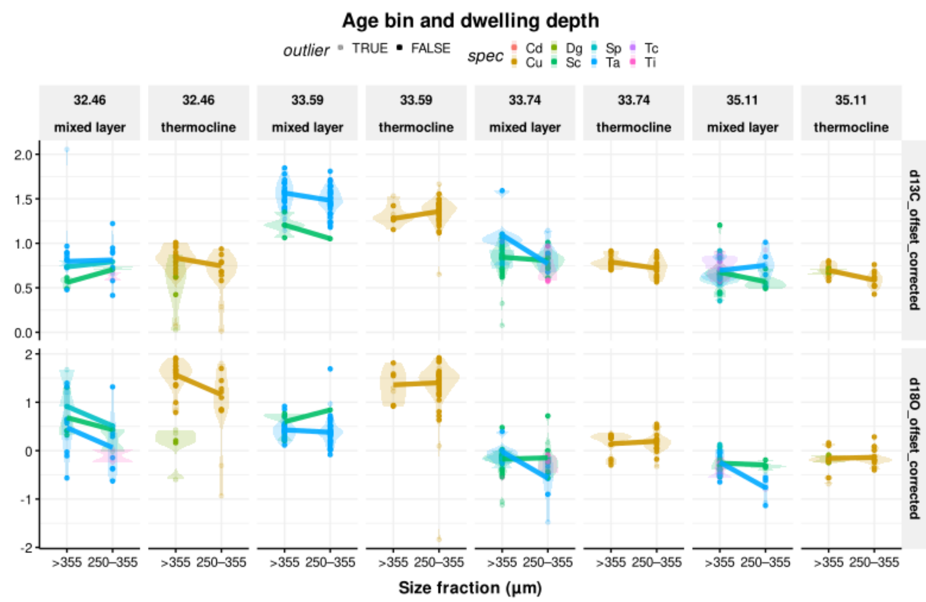

Figure S12. Size fractions were binned for clumped isotope analysis because there was no systematic offset.

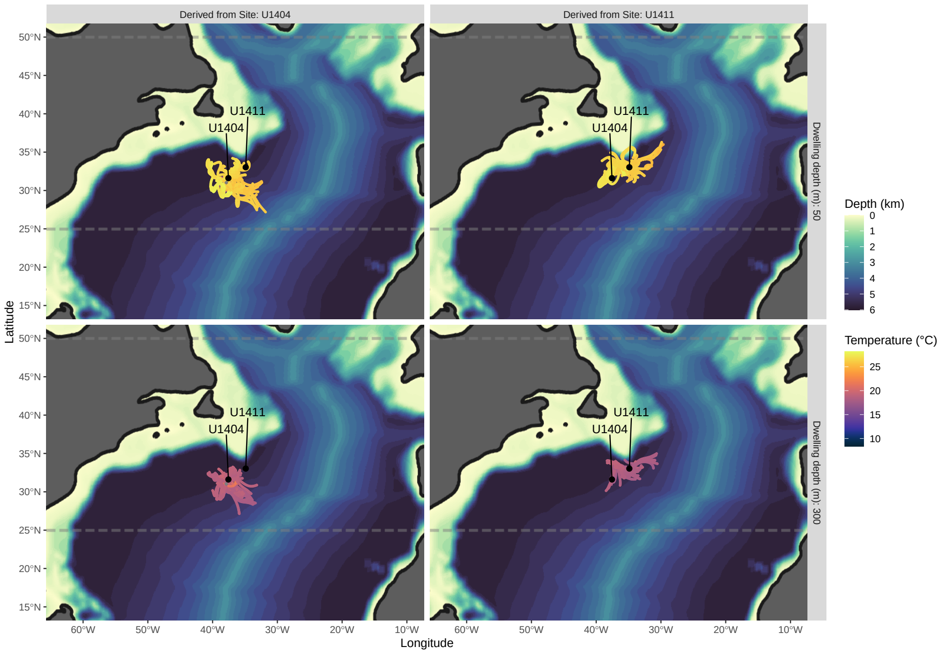

Figure S13. Advective transport for the simulated particles released near the paleolocation of IODP site U1411, with foraminifera dwelling depths of 50 and 300 m (panels). Colour indicates the temperature that the particle is exposed to at that point in time. Also shown is the bathymetry.

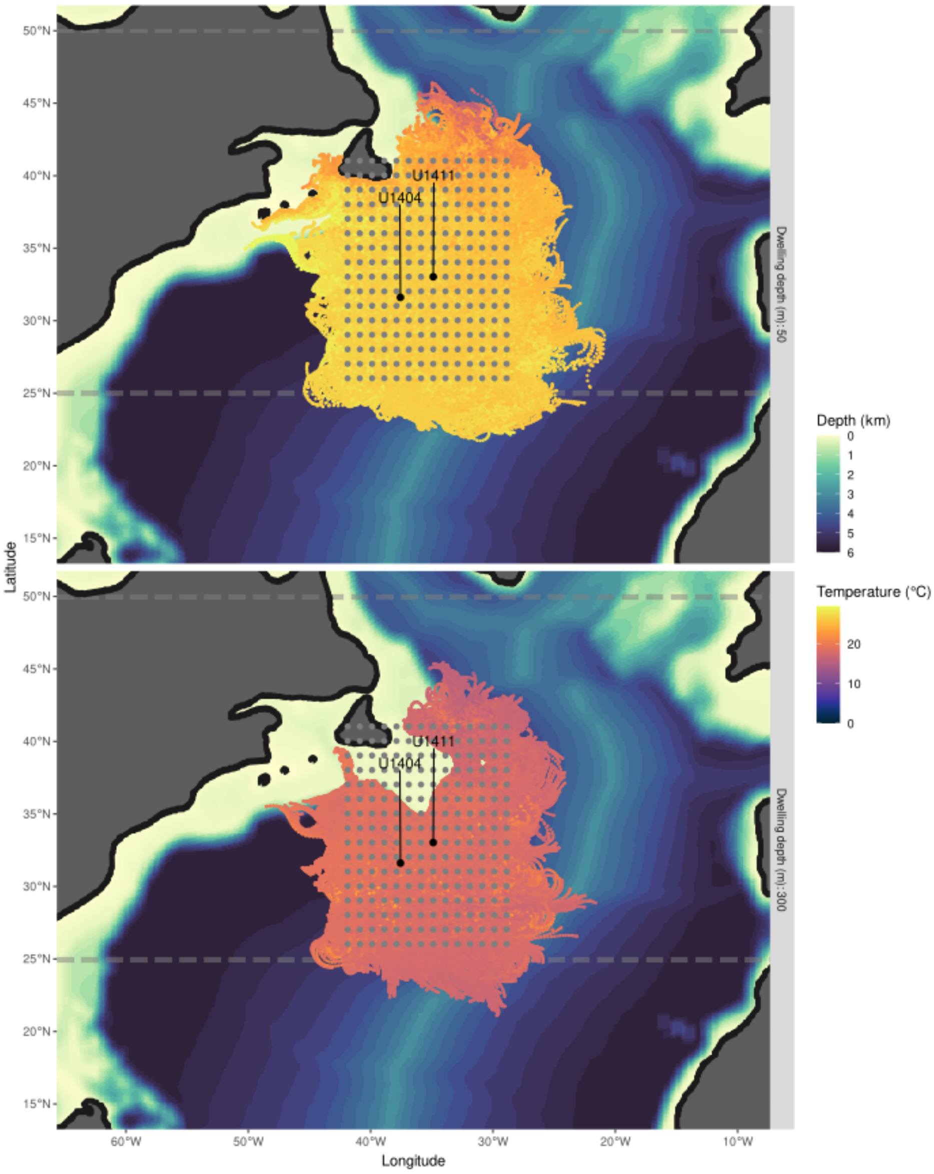

Figure S14. Same as Figure S13 but showing the whole grid of simulated points.

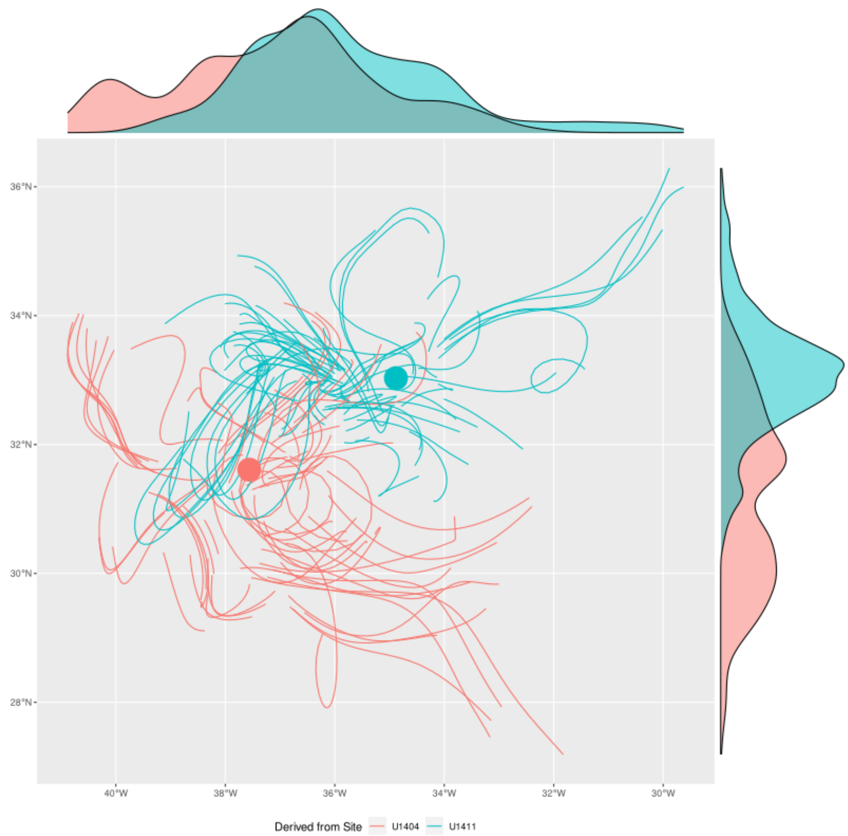

Figure S15. Particles that ultimately arrive at site U1411 show an overlap with those that arrive near site U1404 in longitude and latitude.

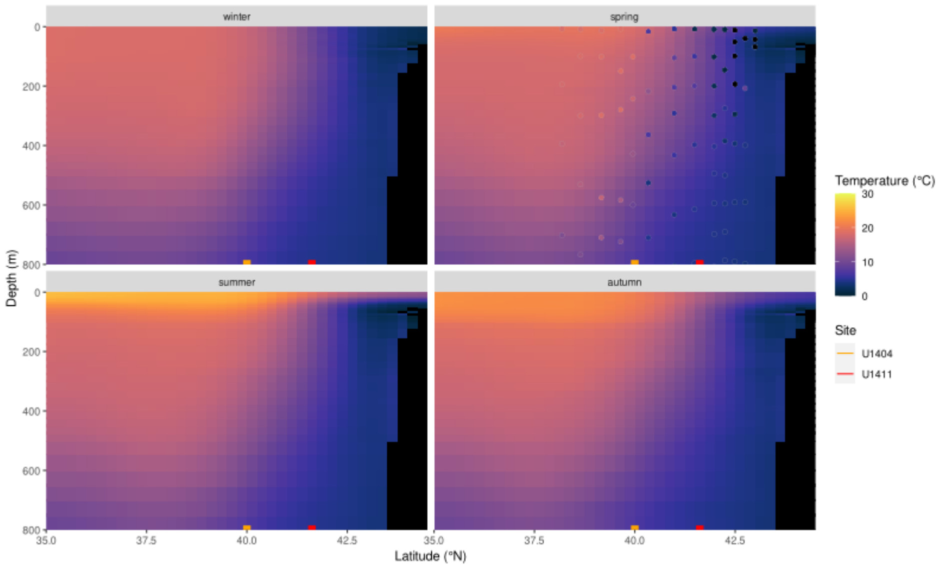

Figure S16. Modern ocean temperature profile of the North Atlantic along the longitude near that of site U1411 (red rectangle) (Locarnini et al., 2019) and site 1404 (orange rectangle) with CTD data (coloured points) from April and May of 1995 between 50.9°E and 49.8°E from WOCE Hydrographic Programme, 2002.